

Synthesis, structural and magnetic properties of ludwigite

$\text{Mn}_{1.32}\text{Ni}_{0.85}\text{Cu}_{0.83}\text{BO}_5$

© S.N. Sofronova¹, E.V. Eremin¹, E.M. Moshkina¹, A.V. Selyanina¹, G.N. Bondarenko², A.V. Shabanov¹

¹Kirensky Institute of Physics, Federal Research Center KSC SB, Russian Academy of Sciences, Krasnoyarsk, Russia

²Institute of Chemistry and Chemical Technology, Federal Research Center KSC SB RAS, Russian Academy of Sciences, Krasnoyarsk, Russia

E-mail: ssn@iph.krasn.ru

Received July 7, 2022

Revised July 7, 2022

Accepted July 9, 2022

Single crystals of $\text{Mn}_{1.32}\text{Ni}_{0.85}\text{Cu}_{0.83}\text{BO}_5$ with the ludwigite structure were obtained by the solution-melt method during spontaneous crystallization. The concentration of copper, manganese and nickel ions was determined by transmission microscopy. Manganese ions are included in compounds in the divalent and trivalent states. The study of temperature and field dependences showed that we have several magnetic transitions. The first transition, associated with the ferrimagnetic ordering of the magnetic moments of parts of the ions, observed in the region of 50 K. In the region of 25 K, a second magnetic transition is observed. Substitution of nickel ions for copper and divalent manganese of better disorder and competition of exchange interactions, which leads to the division of the magnetic system into several magnetic subsystems that are ordered at different temperatures.

Keywords: ludwigites, magnetic interface transition, indirect exchange interactions.

DOI: 10.21883/PSS.2022.11.54200.425

1. Introduction

Transition metal oxyborates, due to geometric features of their structure, can be classified as quasi-low-dimensional compounds [1–7]. In the ludwigite structure (Fig. 1) separate structural elements — triads — can be distinguished [2,3,8]. Triads of the first type are formed by metal ions in sites 4-2-4. Distances between metal ions in sites 2 and 4 are minimal in all known ludwigites. In addition, their octahedra are connected by edges of the base in the same manner as triads 4-2-4 in neighboring cells (along c axis in Fig. 1), resulting in a structure similar to a three-leg ladder (Fig. 2, *a*). Ions in sites 1 and 3 form triads of the second type: 3-1-3, octahedra of these ions are connected by vertices, and distances between ions are the largest possible ones (Fig. 2, *b*). Triads of the second type, being connected along the c axis, form a three-leg ladder as well. Exchange paths between the triads of the first and the second types form triangle groups, that in case of antiferromagnetic interactions results in a strong competition of exchange interactions and occurrence of frustrations.

In Fe_3BO_5 [8] and Cu_2MnBO_5 [9] ludwigites the magnetic system is split into two subsystems connected exactly with the three-leg ladders. In addition, magnetic moments of subsystems are oriented normally in Fe_3BO_5 and at an angle of about 60 degrees in Cu_2MnBO_5 . Ni_2MnBO_5 ludwigites are not as well studied [10–12], as Fe_3BO_5 and Cu_2MnBO_5 , however, these compounds are interesting due to the fact that manganese can be included in them in different valence states. In particular, previously we have obtained

compositions, where in addition to three-valence ions of manganese, four-valence ions of manganese were presented as well [11]. In addition, in $(\text{Ni},\text{Mn})_3\text{BO}_5$ ludwigites the effect of magnetization reversal was found [12]. The study of such effects as noncollinear magnetism, magnetization reversal is interesting not only from the fundamental point of view, but also from the application-oriented point of view, because these effects can be applied for the development of various magnetic devices.

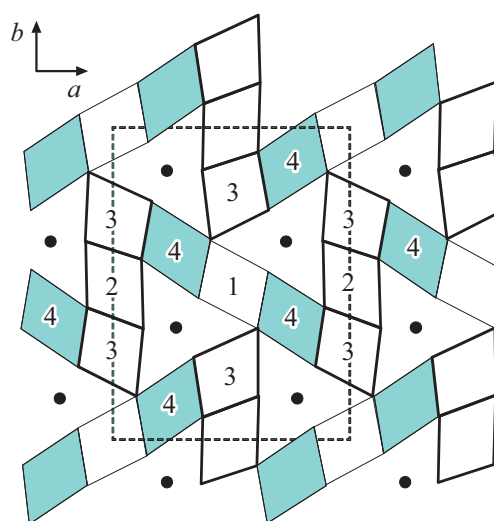


Figure 1. The schematic structure of ludwigite projected along the c axis. Metal ions occupy 4 sites in the centers of oxygen octahedra. Black points show B ions.

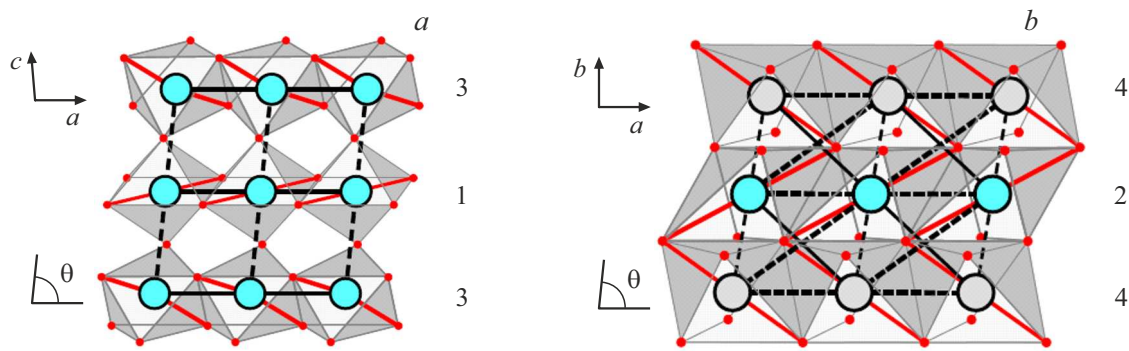


Figure 2. Three-leg ladders formed by triads of the first (a) and the second type (b).

Solid solutions of Ni_2MnBO_5 – Cu_2MnBO_5 are interesting due to the fact that their parent compositions Ni_2MnBO_5 and Cu_2MnBO_5 have rhombic and monoclinic structure, respectively [9–12]. Monoclinic distortions of Cu_2MnBO_5 crystalline structure occur due to the Jahn-Teller effect of copper ions. In Cu_2MnBO_5 magnetic ordering in both subsystems takes place in the region of 90 K. In studying these solid solutions, the issue of sequence of magnetic subsystems ordering is of considerable interest: whether the magnetic subsystems will be ordered at one temperature, as in Cu_2MnBO_5 , or, as in Fe_3BO_5 , the ordering will take place at different temperatures.

In this study we made an attempt to obtain a solid solution of Ni_2MnBO_5 – Cu_2MnBO_5 with high concentration of copper ions. Previously we have obtained three compounds with different compositions, however, it appeared that copper ions were presented in these compounds only in small amounts, even in the case when copper was the predominant element in the solution-melt system [13]. With an increase in the concentration of ions the temperature of magnetic ordering decreased down to 60–75 K (depending on the composition), and at low temperatures in the region of 10 K a feature was detected on ac-susceptibility [14]. Orientation-related study of magnetization has shown that in the region of 60–75 K an ordering of magnetic moments takes place normally to the short axis (c), and in the region of 10 K the ordering of magnetic moments takes place along the short axis (c).

In this paper we present the results of growth experiment to produce a composition with a considerable content of copper ions in $(\text{Ni},\text{Mn},\text{Cu})_3\text{BO}_5$, describe the study of the compound composition by the transmission microscopy method, detailed study of magnetic properties, as well as present an estimate of exchange interactions within the empirical model.

2. Crystal growth

Single crystals of the ludwigite in question, i.e., $(\text{Mn},\text{Ni},\text{Cu})_3\text{BO}_5$, were obtained using the solution-melt method in the spontaneous crystallization mode. In our

previous works [13–14] we made an attempt to obtain a number of compounds from Ni_2MnBO_5 to Cu_2MnBO_5 by substituting nickel ions with copper ions. We took as a basis the solution-melt system to obtain Ni_2MnBO_5 , where CuO copper oxide was added. However, it appeared that copper ions were presented in these compounds only in small amounts, even in the case when copper was the predominant element in the solution-melt system [13]. In this study, taking a solution-melt system as a basis to obtain the Cu_2MnBO_5 ludwigite, we made an attempt to obtain a composition with high copper content.

For this purpose, we took components of the solution-melt system in the following proportion: $\text{Bi}_2\text{Mo}_3\text{O}_{12}:\text{2.66B}_2\text{O}_3:\text{1.4Na}_2\text{O}:\text{1.32Mn}_2\text{O}_3:\text{1.32CuO}:\text{0.1NiO}$.

The solution-melt system with a mass of $m = 83.5$ g was prepared by successive melting together in a platinum crucible ($V = 100$ cm³), at $T = 1100^\circ\text{C}$ of mixtures of powders of Bi_2O_3 – MoO_3 – B_2O_3 , then Mn_2O_3 and NiO . The powder of Na_2CO_3 was added in portions last of all. After the homogenization of the solution-melt system at $T = 1100^\circ\text{C}$ for 3 hours, phase sounding was performed and parameters of the solution-melt system were determined. It was found that high-temperature crystallizing phase in the prepared solution-melt system is the ludwigite phase (in a temperature range of at least 40°C). The saturation temperature was $T_{\text{sat}} = 895^\circ\text{C}$.

After research study the solution-melt system was homogenized again at $T = 1100^\circ\text{C}$ for 3 hours. After that temperature in the furnace was first decreased at a rate of $dT/dt = 200^\circ\text{C/h}$ down to a temperature of $T_{\text{start}} = (T_{\text{sat}} - 5) = 890^\circ\text{C}$, then it decreased slowly, at a rate of $dT/dt = 4^\circ\text{C/day}$. In three days the crucible was removed from the furnace, the solution-melt system was drained off. Grown crystals in the form of elongated black needle-like prisms were separated from the solution-melt residue by etching in a 20% aqueous solution of nitric acid.

3. Study of composition and structure

The obtained single crystals were studied using the TM-4000Plus tabletop scanning electron microscope by

Table 1. Proportion of Ni:Mn:Cu in the solution and in crystals

Proportion of Ni:Mn:Cu in the solution	Proportion of Ni:Mn:Cu in crystals
0.1:2:1	1.02:1.59:1

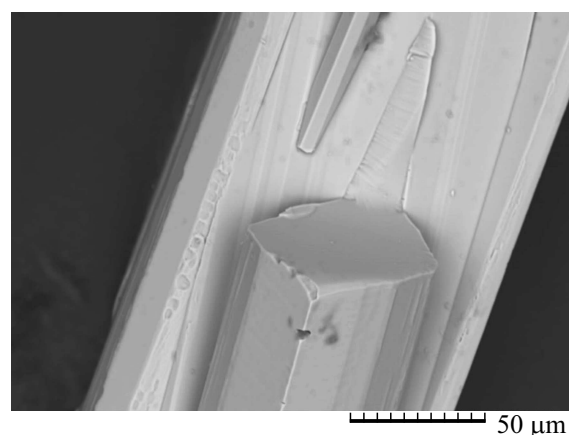
Hitachi at an accelerating voltage of 20 kV. Element charting was carried out using the Bruker XFlash 630Hc x-ray detector. Spectra were analyzed using Quantax70 software. All samples had uniform compositions. To check uniformity, we compared spectra of different areas of crystals for six single crystal samples. Fig. 3 shows the image of the crystals. The proportion of Ni:Mn:Cu in the solution-melt system and in the crystal is shown in Table 1. As can be seen from Table 1, the proportion of Ni:Mn:Cu in the crystal is considerably different from the proportion in the solution-melt system. Despite the content of nickel in the solution, the crystal composition has the number of nickel ions equal to the number of copper ions. The chemical formula of the composition, taking into account the proportion of metal ions in the crystal, is $Mn_{1.32}Ni_{0.85}Cu_{0.83}BO_5$ because nickel and copper ions are included in the compositions with ludwigite structure in a two-valence state. According to the electrical neutrality condition, part of manganese also should be included in the composition in a two-valence state.

The diffraction pattern of the powder was recorded at the Dron-3 X-ray diffractometer, the obtained reflections correspond to the rhombic structure of ludwigite with space group $Pbam$, lattice parameters are $a = 9.256(5) \text{ \AA}$, $b = 12.266(6) \text{ \AA}$, $c = 3.0585(15) \text{ \AA}$. Thus, even with a quite considerable substitution of nickel ions with copper ions, the rhombic structure is kept.

4. Magnetic properties

Magnetic properties of compounds were studied at the PPMS Quantum design setup in the range of temperature of 4–300 K and 0–90 kOe. Single crystal samples, as already mentioned, were needle-like. As a rule, an intensive growth takes place along the shortest crystallographic direction, and we suppose that the crystallographic axis c coincides with the needle direction, however, it was not determined for sure, therefore in the following we shall denote directions of magnetic field application in relation to the crystal, that is along or normal to the needle. Dependencies of magnetization on temperature and field were measured in two directions: along the needle and normal to the needle. Fig. 4 shows magnetization versus temperature curves for a single crystal when a magnetic field is applied along and across the needle in field-cooled (FC) and zero-field-cooled (ZFC) modes.

Several features can be observed on the magnetization curves. In case of the magnetic field applied along the needle, magnetization increases smoothly with temperature

**Figure 3.** Image of the $(Mn,Ni,Cu)_3BO_5$ ludwigite crystal.

decrease down from room temperatures, and near 50 K a quick growth of magnetization starts. In zero field cooling two maxima in the region of 45 and 20 K are observed. In field cooling mode one maximum near 35 K is observed, then the curve demonstrates a „shelf“ with a decrease in temperature (Fig. 4, a). With the field applied normally to the needle the magnetization growth starts near 50 K. Magnetization measured in a zero field cooling and field cooling modes is different in the temperature range of 4–25 K. The magnetization growth with a decrease in temperature is not smooth. At least two features on the curve can be clearly seen.

Also, the dependencies of magnetization versus field for the single crystal sample were measured at the PPMS setup and shown in Fig. 5 and 6. Hysteresis loops are observed on the dependencies of magnetization versus field. When a magnetic field is applied along the needle, the magnetization slightly deviates from the linear law at high temperatures and keeps a nearly unchanged slope, and the coercive field is very low and changes weakly with a decrease in temperature. When a field is applied normally to the needle, the coercive field grows with a decrease in temperature and, in addition, the shape of hysteresis loops changes.

Dependencies of ac-susceptibility versus temperature for polycrystalline samples shown in Fig. 7 demonstrate smooth growth with a decrease in temperature. In the region of 25 K there is a feature, which position does not depend on the alternating field frequency. With further decrease in temperature the susceptibility decreases. The peak of ac-susceptibility near 25 K is quite wide and unsymmetrical. In a temperature range of 4–25 K ac-susceptibility depends on frequency.

Derivatives of the product of susceptibility and temperature (χT) and square magnetization (M^2) with respect to temperature are proportional to heat capacity for systems with different types of magnetic ordering [15]. As can be seen from Fig. 8, $d(\chi T)/dT$ and $d(M^2)/dT$ curves have a feature near 46 K regardless the orientation of the

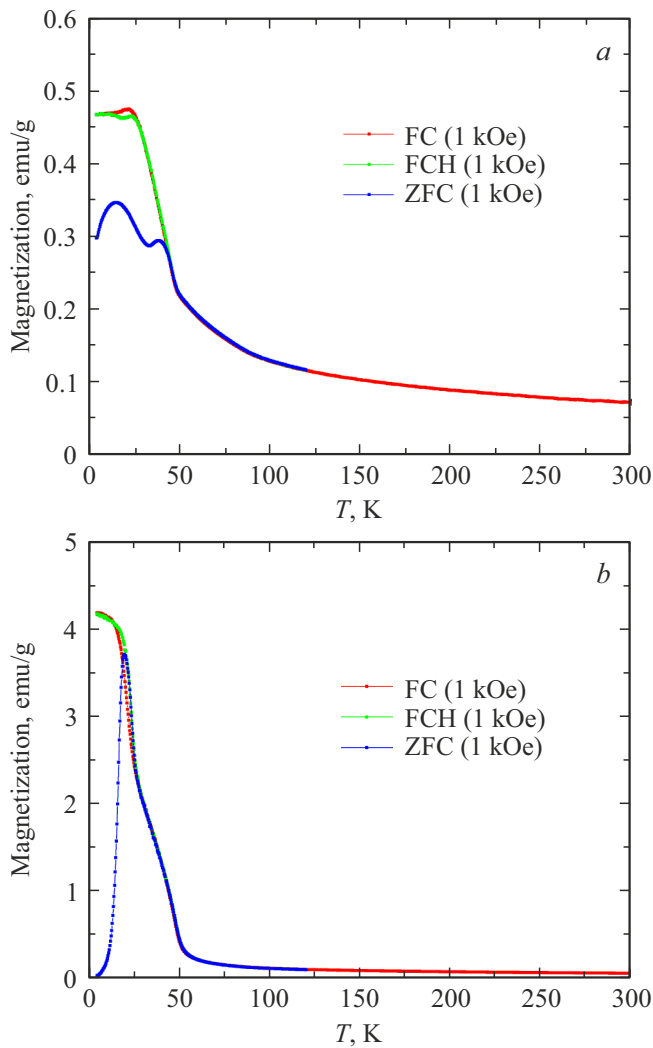


Figure 4. Dependencies of magnetization versus temperature for a single crystal at an applied magnetic field of 1 kOe along (a) and across (b) the needle.

magnetic field. If the field is applied along the needle, the $d(\chi T)/dT$ curve demonstrates a well-defined positive maximum near 35 K, while if the field is applied normal to the needle, there is no well-distinguished feature, although the minimum at 46 K is unsymmetrical, which is probably associated with the fact that there is a feature at 35 K as well. The peak of ac-susceptibility at 25 K matches the maximum of $d(M^2)/dT$ in both directions of field application. The shape of hysteresis loop changes below 25 K, if the field is applied normal to the needle. Probably, a ferromagnetic ordering of one of magnetic subsystems takes place at 25 K. $d(\chi T)/dT$ and $d(M^2)/dT$ curves also have features at low temperatures in the region of 16 K when the field is applied normally to the needle. Probably, the magnetic structure of $Mn_{1.32}Ni_{0.85}Cu_{0.83}BO_5$ is quite complex and there are several subsystems that are ordered at different temperatures.

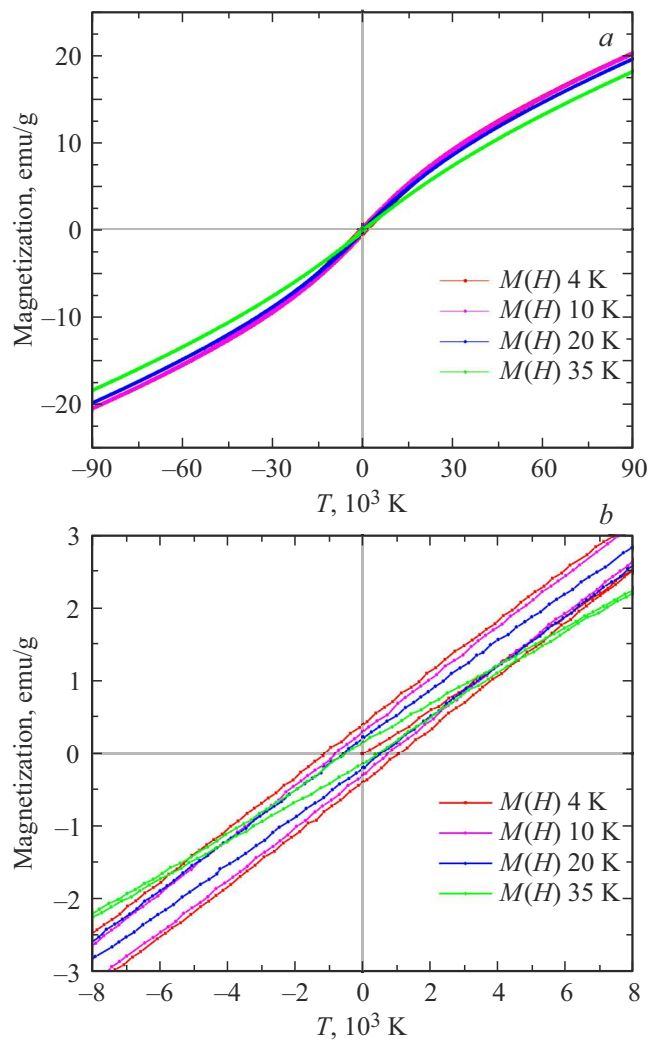


Figure 5. Dependencies of magnetization versus field for a single crystal sample at a field applied along the needle (a). In the smaller scale (b) it can be seen that hysteresis loops have the strongest coercive field of about 1 kOe.

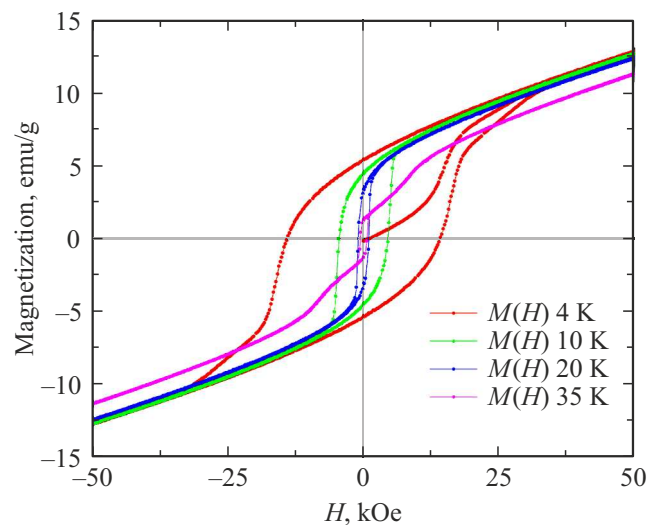


Figure 6. Dependencies of magnetization versus field for a single crystal sample at a field applied across the needle.

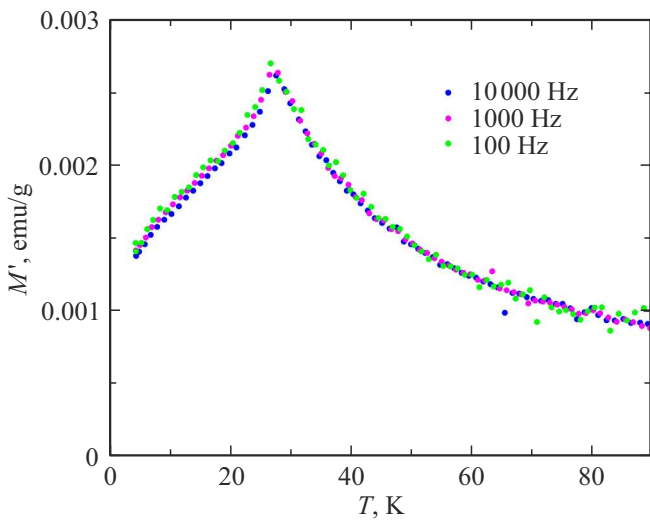


Figure 7. Dependence of ac-susceptibility versus temperature for polycrystalline samples.

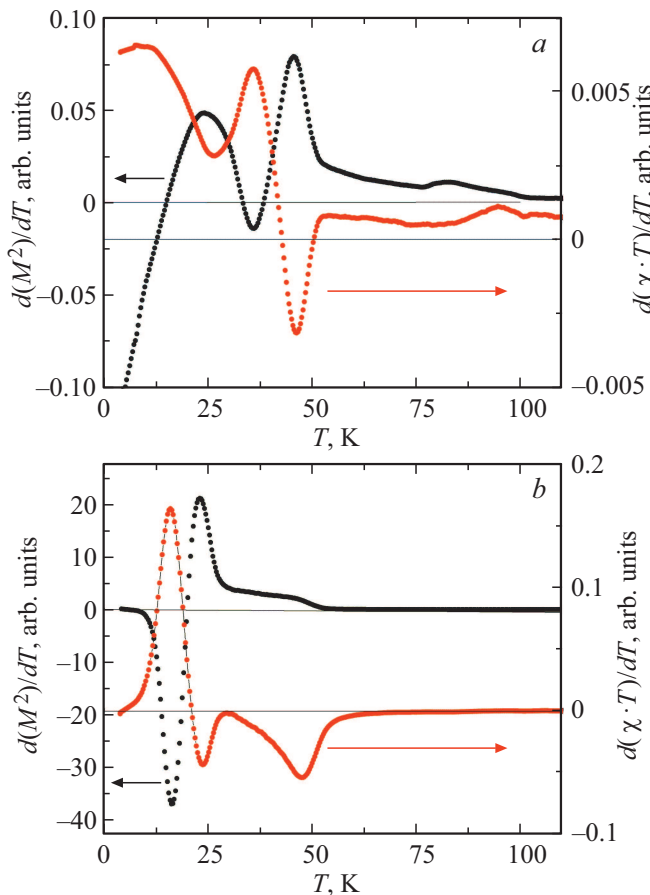


Figure 8. Dependence of $d(\chi T)/dT$ (red curve) and $d(M^2)/dT$ (black curve) versus temperature with a field applied along (a) and across the needle (b).

5. Discussion of results

Previously we studied three compositions where copper content was considerably less than that of man-

ganese: $Mn_{1.04}Ni_{1.85}Cu_{0.11}BO_5$, $Mn_{1.06}Ni_{1.73}Cu_{0.21}BO_5$ and $Mn_{1.22}Ni_{1.57}Cu_{0.21}BO_5$ (sample 1, sample 2, and sample 3, respectively) [14]. Fig. 9 shows dependencies of magnetization versus temperature and field for all three compositions with low copper content and the sample under study when the field is applied normally to the needle. As can be seen from Fig. 9, the temperature of magnetization growth beginning drops with an increase in the concentration of copper in the crystal composition. For compositions with copper content $x > 0.2$ the magnetization is not zero even at a room temperature and there is a well-defined „shelf“. The coercive field for compositions with copper content $x > 0.2$ remains the same, while the hysteresis loop remanence grows with an increase in copper concentration.

The ac-susceptibility curve of compositions 1 and 2 polycrystalline samples has a feature, i.e., a small plateau in the region of 60–75 K, and in the region of 10 K in compo-

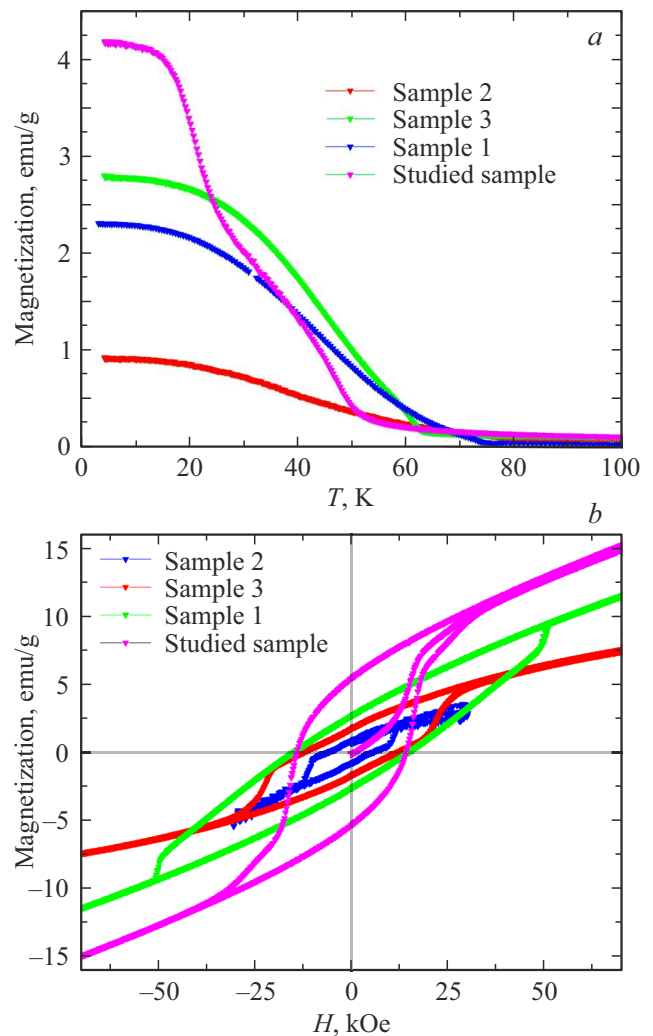


Figure 9. Dependencies of magnetization versus temperature (a) and field (b) for three compositions with low copper content and the sample under study when the field is applied normally to the needle.

sitions 1 and 2 a sharp peak is observed (Fig. 10) [14]. In the sample under study the sharp peak on the ac-susceptibility curve is shifted towards higher temperatures (about 30 K for the sample under study), and the feature in the region of 50 K is smoothed to a significant extent.

Thus, an increase in copper concentration results in a stronger chemical disordering. In addition, in the sample under study and in composition 3 ($\text{Mn}_{1.22}\text{Ni}_{1.57}\text{Cu}_{0.21}\text{BO}_5$), to meet the condition of electrical neutrality, a part of manganese should be in a two-valence state, that results in stronger chemical disordering as well.

In our previous studies we estimated indirect exchange interactions in Ni_2MnBO_5 and Cu_2MnBO_5 compounds [9,10] within the model of indirect exchange interactions on the basis of the Anderson–Zavatsky model [16–19]. Since the structure of Cu_2MnBO_5 is monoclinic, a part of exchange paths changes because of structural distortions (Fig. 2), the number of different exchange interactions in Cu_2MnBO_5 increases as compared with Ni_2MnBO_5 (Table 2).

Table 2, in addition to exchange interactions of Ni_2MnBO_5 , Cu_2MnBO_5 ludwigites, shows the exchange interactions calculated for Mn_3BO_5 ludwigite, because in the sample under study manganese appears in the two-valence state. As can be seen from Table 2, the most strong difference in Ni_2MnBO_5 and Cu_2MnBO_5 is between the exchange interactions 2-4, both 90- and 180-degree. In Ni_2MnBO_5 180-degree exchange interactions 2-4 are very weak, while in Cu_2MnBO_5 , in contrast, the 90-degree exchange interactions 2-4 are weak. Thus, copper ions in site 2 in Ni_2MnBO_5 will result in the occurrence of antiferromagnetic interactions in the subsystem and a stronger competition inside the subsystem 4-2-4. In addition, the exchange interaction 1-3 in the subsystem 3-1-3 has different signs in copper and nickel ludwigites, therefore, in case of substitution the disordering will be increased and the competition will be stronger.

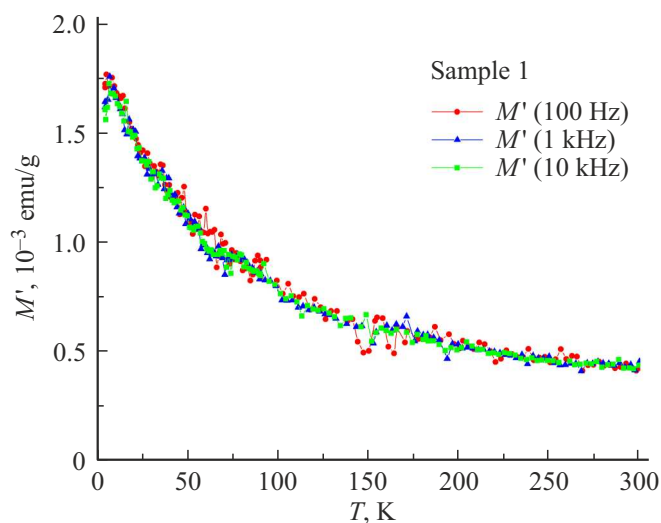


Figure 10. Dependence of ac-susceptibility versus temperature for polycrystalline samples with composition 1.

Table 2. Exchange interactions in Ni_2MnBO_5 , Cu_2MnBO_5 , and Mn_3BO_5 ludwigites

Indirect exchange interactions	J (K) Ni_2MnBO_5 [10]	J (K) Cu_2MnBO_5 [9]	J (K) Mn_3BO_5
4-4 (90°)	-1.8	-5.5	
1-1, 2-2, 3-3 (90°)	5.6	7.9	-5.7
4-2 (90°)	-5.1	0.0	-7.2
4-2 (180°)	0.6	-8.3 1.7	-1.18
4-3 (90°)	-4.6	-0.77 -5.0	-5.4
4-1 (90°)	-4.6	0.1 -6.0	-5.4
4-3 (117°)	-1.0	-2.7 -1.8	-0.24
1-3 (121°)	-1.8	6.83	-1.9
2-3 (90°)	5.6	15.6 7.9	-4.4

The appearance of two-valence manganese at the sites of two-valence ions of copper and nickel results in the emergence of antiferromagnetic interactions in the ion chains 1-1, 2-2, 3-3, as well as between ions in site 2 and 3, that are ferromagnetic in both parent compositions: Ni_2MnBO_5 and Cu_2MnBO_5 . Thus, in case of substitution of nickel ions with ions of two-valence manganese, the ferromagnetic ordering along the short axis c , which is observed in Cu_2MnBO_5 , may be disturbed. In case of substitution of nickel ions with ions of copper and two-valence manganese, the competition of exchange interactions is strengthened considerably both inside magnetic subsystems and between them, which results in a decrease in the temperature of magnetic ordering, emergence of several magnetic subsystems that are ordered at different temperatures.

6. Conclusion

Using the method of solution-melt system with spontaneous crystallization we have managed to obtain single crystals of $\text{Mn}_{1.32}\text{Ni}_{0.85}\text{Cu}_{0.83}\text{BO}_5$ with ludwigite structure where the concentration of copper ions is comparable with the concentration of nickel ions. Despite the high content of copper ions, the crystalline structure remains rhombic as that of Ni_2MnBO_5 . The concentration of copper, manganese, and nickel ions was studied by the method of transmission microscopy, the formula of the compound was refined. Due to the condition of electrical neutrality, manganese ions are included in the composition

in two-valence and three-valence states. The detailed study of magnetic properties has shown that several magnetic transitions are observed. The first transition related to ferromagnetic ordering of magnetic moments of a part of ions is observed in the region of 50 K, and yet another magnetic subsystem is ordered in the region of 25 K. The substitution of nickel ions with copper and two-valence manganese strengthens chemical disordering and competition of exchange interactions, that results in a break down of the magnetic system into several magnetic subsystems that are ordered at different temperatures.

Acknowledgments

The authors would like to thank M.S. Molokeev for the refinement of lattice parameters of the crystalline structure.

Funding

The study was done with financial support from the Russian Foundation for Basic Research, Government of Krasnoyarsk Territory and the Krasnoyarsk Regional Fund of Science within scientific project No. 20-42-240011. The research was carried out using the equipment provided by the Krasnoyarsk Regional Center for Collective Use.

Conflict of interest

The authors declare that they have no conflict of interest.

References

- [1] L.N. Bezmaternykh, S.N. Sofronova, N.V. Volkov, E.V. Eremin, O.A. Bayukov, I.I. Nazarenko, D.A. Velikanov. *Phys. Status Solidi B* **249**, 8, 1628 (2012).
- [2] E. Bertaut. *Acta Crystollogr.* **3**, 473 (1950).
- [3] H. Neuendorf, W. Gunser. *J. Magn. Magn. Mater.* **173**, 117 (1997).
- [4] J.C. Fernandes, R.B. Guimarães, M.A. Continentino, H.A. Borges, J.V. Valarelli, Alex Lacerda. *Phys. Rev. B* **50**, 16754 (1994).
- [5] A. Arauzo, N.V. Kazak, N.B. Ivanova, M.S. Platonov, Y.V. Knyazev, O.A. Bayukov, L.N. Bezmaternykh, I.S. Lyubutin, K.V. Frolov, S.G. Ovchinnikov, J. Bartolomé. *J. Magn. Magn. Mater.* **392**, 114 (2015).
- [6] A.M. Kadomtseva, Yu.F. Popov, G.P. Vorob'ev, A.P. Pyatakov, S.S. Krotov, K.I. Kamilov, V. YuIvanov, A.A. Mukhin, A.K. Zvezdin, A.M. Kuz'menko, L.N. Bezmaternykh, I.A. Gudim, V.L. Temerov. *Low Temp. Phys.* **36**, 511 (2010).
- [7] S.N. Sofronova, N.V. Kazak, E.V. Eremin, E.M. Moshkina, A.V. Chernyshov, A.F. Bovina. *J. Alloys Comp.* **864**, 158200 (2021).
- [8] P. Bordet, E. Suard. *Phys. Rev. B* **79**, 144408 (2009).
- [9] E. Moshkina, C. Ritter, E. Eremin, S. Sofronova, A. Kartashev, A. Dubrovskiy, L. Bezmaternykh. *J. Phys. Condens. Matter*, **29**, 24, 245801 (2017).
- [10] S. Sofronova, E. Moshkina, I. Nazarenko, A. Veligzhanin, M. Molokeev, E. Eremin, L. Bezmaternykh. *J. Magn. Magn. Mater.* **465**, 201 (2018).
- [11] L.N. Bezmaternykh, E.M. Kolesnikova, E.V. Eremin, S.N. Sofronova, N.V. Volkov, M.S. Molokeev. *J. Magn. Magn. Mater.* **364**, 55 (2014).
- [12] E. Moshkina, S. Sofronova, A. Veligzhanin, M. Molokeev, I. Nazarenko, E. Eremin, L. Bezmaternykh. *J. Magn. Magn. Mater.* **402**, 69 (2016)
- [13] E. Moshkina, A. Bovina, M. Molokeev, A. Krylov, A. Shabanov, A. Chernyshova, S. Sofronova. *Cryst. Eng. Commun.* **23**, 5624 (2021)
- [14] A. Kartashev, E. Eremin, E. Moshkina, M. Molokeev, S. Sofronova. *J. Magn. Magn. Mater.* **545**, 168747 (2022).
- [15] M.E. Fisher. *Phil. Mag.* **7**, 1731 (1962).
- [16] O.A. Bayukov, A.F. Savitskii. *Phys. Status Solidi B* **155**, 249 (1989).
- [17] O.A. Bayukov, A.F. Savitsky. *FTT* **36**, 1923 (1994) (in Russian).
- [18] P.W. Anderson. *Phys. Rev.* **115**, 2 (1959).
- [19] M.V. Eremin. *FTT* **24**, 423 (1982) (in Russian).